European Journal of Molecular Biotechnology

Issued since 2013

E-ISSN 2409-1332
2022. 10(1). Issued once a year

Journal is indexed by: **Chemical Abstracts Service** (USA), **CiteFactor** – Directory of International Reseach Journals (Canada), **Cross Ref** (UK), **EBSCOhost Electronic Journals Service** (USA), **Global Impact Factor** (Australia), **Journal Index** (USA), **Electronic scientific library** (Russian Federation), **Open Academic Journals Index** (USA), **Sherpa Romeo** (Spain), **ULRICH's WEB** (USA).

All manuscripts are peer reviewed by experts in the respective field. Authors of the manuscripts bear responsibility for their content, credibility and reliability.

Editorial board doesn't expect the manuscripts' authors to always agree with its opinion.

Postal Address: 1717 N Street NW, Suite 1, Washington, District of Columbia 20036

Website: https://ejmb.cherkasgu.press
E-mail: office@cherkasgu.press

Founder and Editor: Cherkas Global University

Release date 15.09.22
Format 21 × 29,7/4.

Headset Georgia.

Order № 23.

European Journal of Molecular Biotechnology

2022

Is. 1

C O N T E N T S

Articles

Published in the USA
European Journal of Molecular Biotechnology
Issued since 2013.
E-ISSN: 2409-1332
2022. 10(1): 3-7

DOI: 10.13187/ejmb.2022.1.3
https://ejmb.cherkasgu.press

Articles

Hexagonal I_h Ice and Water Clusters. Mpemba Effect. Entropic Parameters of Hydrogen Bonds

Ignat Ignatov [a, *], Georgi Gluhchev [b], Fabio Huether [c], Mario T. Iliev [d], Christos Drossinakis [e], Teodora P. Popova [f], Alexander I. Ignatov [a]

[a] Scientific Research Center of Medical Biophysics (SRCMB), Sofia, Bulgaria
[b] Bulgarian Academy of Sciences (BAS), Sofia, Bulgaria
[c] EVODROP AG, Zurich, Brüttisellen, Switzerland
[d] Faculty of Physics, Sofia University St. Kliment Ohridski, Sofia, Bulgaria
[e] IAWG – INTERNATIONALE Akademie für Wissenschaftliche Geistheilung, Frankfurt, Germany
[f] University of Forestry, Faculty of Veterinary Medicine, Sofia, Bulgaria

Abstract

The importance of ice in sustaining life on our planet is difficult to underestimate. Ice significantly influences the living conditions and activities of plants, animals, and various human activities. By covering water and ice, due to its low density, plays the role of a floating screen in nature, protecting rivers and reservoirs from further freezing and preserving the life lives of underwater inhabitants.

The utilization of ice for various purposes (snow retention, construction of ice crossings and isothermal warehouses, ice filing of storage, and mines) constitutes the subject of several branches of hydro-meteorological and engineering sciences.

Natural ice is used for storing and cooling food products and biological and medical preparations, for which it is specifically produced and harvested, and melt water obtained during ice melting.

The study of ice, including its hexagonal structure (Ice I_h), highlights its intricate properties. Furthermore, investigations of the Mpemba effect, where warm (37-60°C) and hot water (>60°C) freeze faster than cold water, shed light on the interplay between entropy and hydrogen bond energies. Understanding these phenomena contributes to scientific knowledge and impacts practical applications in various industries and environmental contexts.

In summary, the importance of ice transcends mere natural phenomena, deeply intertwining with human activities, scientific endeavors, and sustenance of life across the planet, serving as a cornerstone in various ecological and industrial domains.

Keywords: hexagonal, water clusters, ice, entropy.

1. Introduction

At the corners of the crystalline lattice of ice, the oxygen (O) atoms are symmetrically arranged. They form regular hexagons. Hydrogen atoms occupy different positions and bond with

* Corresponding author
E-mail addresses: mbioph@abv.bg (I. Ignatov)

the oxygen atoms through hydrogen bonds. Figure 1 illustrates a hexagonal structure of the ice (Ignatov, Mosin, 2014).

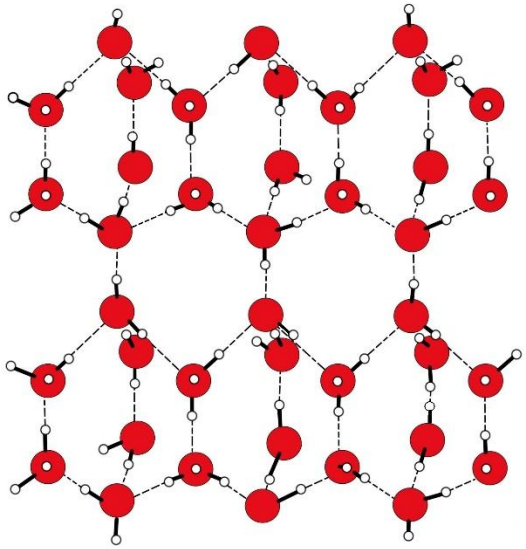

Fig. 1. Hexagonal structure of ice I_h

Research reveals that the $(H_2O)_6$ cage and $(H_2O)_{20}$ dodecahedron water clusters have a hydrogen bond topology that can be described in liquid and ice phases. The two clusters exhibit approximately the same hydrogen bond arrangement in water's liquid and solid phases (Gao et al, 2021; Iliev et al., 2023). $(H_2O)_6$ features 27, and $(H_2O)_{20}$ has 30 026 symmetry-distinct hydrogen bonds (Kuo et al., 2001).

The study used the discrete evaporation of water drops with the spectral methods NES and DNES clusters (Antonov, 1995; Todorova, Antonov, 2000; Ignatov, Valcheva, 2023).

2. Materials and Methods

Spectral methods Non-equilibrium energy spectrum (NES) and Differential non-equilibrium energy spectrum (DNES)

According to (Luck, 1980), the water molecules are bound with the energy of hydrogen bonds with energy (-E). When the water molecules are not connected with hydrogen bonds, the energy is E=0. This is recognized as the two-state model of Luck (Kontogeorgis et al., 2022; Vega, Lovell, 2016).

In a specific volume of water and our experiments, we study water drops the water, interlinked by van der Waals forces and electromagnetic hydrogen bonds, is considered an associated liquid (Antonov, 1995).

The investigation of water drops was performed in a hermetic camera with an optic system to research the wetting angle θ (Antonov et al., 1989). The parameters of the wetting angle are connected with the parameters of hydrogen bonds with a formula (Todorov et al., 2008; Todorov et al., 2010).

$\Theta = \arccos(-1+bE)$, where $b = I(1+\cos\theta_o)/C\gamma o$ (1)

The range of the parameters of the hydrogen bonds is the following:

E=(-0.0912)-(-0.1387) eV; 736-1117 cm^{-1}; λ = 8.9 – 13.6 μm

In (1) θ is the wetting angle, and b is a temperature-dependent parameter. E is the energy of hydrogen bonds between one water molecule's oxygen atom and another's hydrogen (Gramatikov et al., 1992; Kumbhakkhane et al., 2013).

The function f(E) is estimated as an *energy distribution spectrum*. A non-equilibrium process of evaporation of water droplets is the energy spectrum of water. The value of NES and DNES is eV^{-1}. (Antonov, 1995; Todorova, Antonov, 2000; Mehandjiev et al., 2023).

DNES is the difference between the NES spectrum of the water sample and the NES of a control water sample.

Δf(E)=f(water sample)-f(control water sample) (2)

DNES is studied in eV^{-1}

Note: In our experiments, the water temperature is 1°C because the NES and DNES methods of research are with liquid water.

3. Results and discussion

3.1. Mathematical problem – a hexagonal structure of the ice.

One of the co-authors, Gluhchev, created the following mathematical problem. The regular hexagon is the only regular polygon whose distance from the center to any vertex equals the distance between two adjacent vertices. Let's consider a regular polygon with center point O and points P and Q as two adjacent vertices. We'll denote the side length as R and α as the central angle ORQ, equal to 360°/p. Let point M be the midpoint of side PQ. From the right triangle OMR, we have:

$MP/OP = R/(2OP) = \sin(\alpha/2) = \sin(360^o/2n)$

$OP = R/2\sin(360^o/2n)$

За OP = R the result is

$R = R/2\sin(360^o/2n)$

or

$\sin(360^o/2n) = 1/2$ или $360^o/2n = 30^o$ или $n = 6$.

With this, the theorem has been proven.

Corollary: If p < 6, then α > 60°, and OR < R; if p > 6, then α < 60°, and OR > R.

Hypothesis: In a planar ring-like structure of a water cluster with p < 6, having an H atom at the center is impossible due to the limitation of permissible distances between atoms. With p > 6, the distance from the central atom to the atoms at the vertices is greater than the distance between two adjacent atoms of the polygon, resulting in a weaker bond.

Conclusion: A hexagon is the most stable configuration of a planar cluster, representing a regular polygon with an atom at the center.

In water, hydrogen bonds are an example of negative entropy in freezing water. At low temperatures, water forms stable structures of hydrogen bonds, leading to a negative entropy of these bonds.

Negative entropy indicates an organized and structured system.

The results for different types of hexagonal water clusters for the wavenumbers $\tilde{\nu}$ are 929, 992, 1117, 3072, and 3171 cm^{-1}. There are wavenumbers of hexagonal water clusters with different combinations of water molecules for n=6 (Table 1) (Heine, 2013).

Table 1. Wavenumbers of hexagonal water clusters with different combinations of water molecules for n=6

Combinations Hexagonal water clusters	$\tilde{\nu}$ (cm^{-1})	$\tilde{\nu}$ (cm^{-1})	$\tilde{\nu}$ (cm^{-1})	$\tilde{\nu}$ (cm^{-1})	$\tilde{\nu}$ (cm^{-1})
1st combination	929	992	1117	3072	3171
2d combination	929	992	1117	3072	
3rd combination	929	992	1117		
4th combination	929		1117		
5th combination			1117		

Table 1 shows that in the combinations of water clusters exists a peak at $\tilde{\nu}$=1117 cm^{-1}. This peak corresponds with the energy of hydrogen bonds between water molecules.

3.2. Entropy. Effect of Mpemba

In 1963, Tanzanian high school student Erasto Mpemba observed an intriguing phenomenon. Hot water freezes faster than cold water. This phenomenon, known as the "Mpemba effect," was actually noted much earlier by historical figures such as Aristotle, Francis Bacon, and Rene Descartes. Numerous independent experiments have since confirmed this unusual property of water.

In 1969, experiments were conducted with the freezing rates of water. For the freezing rate of water at 42°C the result was 3 h 25 min 30 sec. For the freezing rate of water at 18°C the result was 4 h 40 min 15 sec (Kell, 1969).

From the perspective of one of the co-authors, Ignatov lies in the concept of the Differential Non-equilibrium Energy Spectrum (NES). Hot water possesses a DNES with a lower average energy at room temperature. As a result, the hot water requires less energy to initiate the structuring of crystals and undergo the freezing process.

According to one of the co-authors, Ignatov, the manifestation of the Mpemba effect is associated with the state of water's entropy depending on the energy of the hydrogen bonds.

According to one of the co-authors, Ignatov, the manifestation of the Mpemba effect

The result of DNES from 20° to 1°C is

$\Delta E = (-0.1160) - (-0.1120) = - 0.004$ eV

The result of ΔS from 20° to 1°C is

$\Delta S = \Delta E/T = -0.004/19 = -0.00026$ eV/K $= -21.10^{-5}$ eV/K

The result of DNES from 100° to 1°C is

$\Delta E = (-0.1120) - (-0.1160) = +0.004$ eV

The result of ΔS from 90° to 1°C is

$\Delta S = \Delta E/T = 0.004/99 = +0.00008$ eV/K $= +4.04.10^{-5}$ eV/K

The theoretical entropy value of ice I_h is $\Delta S = 3.493.10^{-5}$ eV/K (Cherodov, 2020). When water freezes, the entropy aligns with that ice. The obtained experimental results correspond with the theoretical calculations. In absolute terms, the entropy change is 5.2 times greater from 20° to 1°C than from 90° to 1°C. In entropy terms, the change in entropy is smaller when warm water freezes compared to when cold water does

4. Conclusion

The study delves into various aspects of water properties, mainly focusing on hydrogen bonds and their influence on ice formation and the Mpemba effect. Several crucial findings emerged by exploring the spectral methods NES and DNES and the mathematical insights into hexagonal structures of liquid and solid phases of water.

1. Hydrogen Bonds and Hexagonal Ice Structures. Investigating the hydrogen bond topology in water clusters $(H_2O)_6$ and $(H_2O)_{20}$ provided compelling evidence of their similarity in liquid and ice phases. The regular hexagonal structure of ice (I_h) demonstrated a stable arrangement of oxygen and hydrogen atoms, revealing insights into the organization of water molecules.
2. The Mpemba Effect and Differential Energy Spectrum (DNES). The Mpemba effect, where warm and hot water freezes faster than cold water, remains a fascinating scientific observation. The DNES spectrum suggested a lower average energy in hot water, correlating with faster crystalline structuring and freezing.
3. Mathematical Insights into Hexagonal Structures. Mathematical deductions affirmed the stability of the hexagonal structure in planar water clusters. This analysis added a theoretical dimension to understanding water's molecular arrangements, highlighting the intricate stability within water clusters.
4. Entropy and Ice Formation. Entropy measurements revealed intriguing patterns during ice formation, particularly aligning with the theoretical entropy values of ice I_h.
5. The comparison of entropy changes from different temperatures demonstrated intriguing variations in entropy alterations during water freezing.

This study amalgamates spectral methods, mathematical deductions, and empirical observations to deepen our understanding of water's molecular behavior, especially concerning hydrogen bonds, ice formation, and the Mpemba effect. These findings provide crucial insight into fundamental properties governing water's behavior in various environmental and scientific contexts.

References

Antonov et al., 1989 – *Antonov, A., Yuskesselieva, L., Teodossieva, I.* (1989). Influence of ions on the structure of water under conditions far away from equilibrium. *Physiologie*. 26: 2552.

Antonov, 1995 – *Antonov, A.* (1995). Research of the non-equilibrium processes in the area of allocated systems. Dissertation thesis for degree "Doctor of Physical Sciences", Blagoevgrad, Sofia, 1-255.

Cherodov, 2020 – *Cherodov, V.N.* (2020). Entropy model of hexagonal ice crystals. *Vestnik Syktyvkarskogo Universiteta. Serya 1: Matematika, Mekhanika, Informatika*. 2 (54): 5-14.

Gao et al., 2021 – *Gao, Y., Fang, H., Ni, K.* (2021). A hierarchical clustering method of hydrogen bond networks in liquid water undergoing shear flow. *Scientific Reports*. 11: 9542.

Gramatikov et al., 1992 – *Gramatikov, P., Antonov, A., Gramatikova, M.* (1992). Study of water's properties and structure variations under the stimulus of outside influence. *Frezenius Z. Anal. Chem*. 343: 134-135.

Heine et al., 2013 – *Heine, N., Fagiani, M. R., Rossi, M. et al.* (2013). Isomer-selective detection of Hydrogen-bond vibrations in the protonated water hexamer. *J. Am. Chem. Soc*. 135(22): 8266-8273.

Ignatov, Mosin, 2014 – *Ignatov, I., Mosin, O. V.* (2014). Nature of hydrogen bonds in liquids and crystals. Ice Crystal Modifications and Their Physical Characteristics. *Journal of Medicine, Physiology and Biophysics*. 4: 58-80.

Ignatov, Valcheva, 2023 – *Ignatov, I., Valcheva, N.* (2023). Physicochemical, isotopic, spectral, and microbiological analyses of water from glacier Mappa, Chilean Andes. *J. Chil. Chem. Soc*. 68(1): 5802-5906.

Kell, 1969 – *Kell, S.G.* (1969). The freezing of hot and cold water. *Am. J. Phys*. 37: 564-565.

Kontogeorgis et al., 2022 – *Kontogeorgis, G.M., A. Hoster, A., Kottaki, N. et al.* (2022). Water structure, properties, and some applications – a review. *Chemical Thermodynamics and Thermal Analysis*. 6: 100053.

Kumbharkhane et al., 2013 – *Kumbharkhane, A., Joshi, Y. S., Mehrotra, S. C. et al.* (2013). Study of hydrogen bonding and thermodynamic behavior in water–1,4-dioxane mixture using time domain reflectometry. *Physic B: Condensed Matter*. 421: 1-7.

Kuo et al., 2001 – *Kuo et al.* (2001). On using graph invariants to efficiently generate hydrogen bond topologies and predict the physical properties of water clusters and ice. *J. Chem. Phys*. 114: 2527.

Luck, 1980 – *Luck, W.* (1980). A model of hydrogen-bonded liquids. *Angewandte Chemie*. 19: 28-41.

Mehandjiev et al., 2023 – *Mehandjiev, D., Gluhchev, G., Neshev. N. et al.* (2023). History-dependent hydrogen bonds energy distributions in NaCl aqueous solutions undergoing osmosis and diffusion through a ceramic barrier. *J Chem Technol Metall*. 58(2): 340-346.

Todorov et al., 2008 – *Todorov, S., Damianova, A., Sivriev, I. et al.* (2008). Water energy spectrum method and investigation of the variations of the H-bond structure of natural waters. *Comptes Rendus de l 'Academie Bulg. des Sci*. 61: 857-862.

Todorov et al., 2010 – *Todorov, S., Damianova, A., Antonov, A. et al.* (2010). Investigations of natural waters spectra from the Rila mountain national park lakes. *Comptes Rendus de l 'Academie Bulg. des Sci*. 63: 555-560.

Todorova, Antonov, 2000 – *Todorova, L., Antonov, A.* (2000). Note on the drop evaporation method for studying water hydrogen bond distribution: An Application to filtration. *Comptes Rendus de l 'Academie Bulg. des Sci*.

Vega, Lovell, 2016 – *Vega, L.F., Lovell, F.* (2016). Review, insights into applying molecular-based equations of state of water and aqueous solutions. *Fluid Ph. Equilib*. 416: 150-173.

Published in the USA
European Journal of Molecular Biotechnology
Issued since 2013.
E-ISSN: 2409-1332
2022. 10(1): 8-14

DOI: 10.13187/ejmb.2022.1.8
https://ejmb.cherkasgu.press

Water Treated with Permanent Magnetic Field. Effects of Potassium Carbonate

Ignat Ignatov [a, *]

[a] Scientific Research Center of Medical Biophysics (SRCMB), Sofia, Bulgaria

Abstract

Scientific studies indicate that the quality of milk and dairy products from cows, sheep, and goats can be enhanced by improving the properties of water. The author introduces a plastic container holding 1000 liters or 1 ton of water subjected to a constant magnetic field. Additionally, potassium carbonate is dissolved in the container. The alkaline environment affects the acidity of the animals' stomachs and provides protection against diseases.

Studies and analyses have been conducted on the effects on water using potassium carbonate and a constant magnetic field. The spectral methods Non-equilibrium Energy Spectrum (NES), Differential Non-equilibrium Energy Spectrum (DNES), and Infrared Fourier Spectral Analysis were applied for the studies.

Deionized water with a volume of 1 liter was used as the model system. The results are extrapolated for a volume of 1000 liters or 1 ton of drinking water.

The obtained water complies with Ordinance No 9/2001, Official State Gazette, issue 30, and Decree No 178/23.07.2004 of Council of Ministers, Bulgaria. The two documents are connected with the quality of water for drinking and household purposes.

Potassium, carbonate, and bicarbonate ions are not included in the regulation. They are not subject to any limit or restriction.

Keywords: magnetic water, potassium carbonate, water, domestic animals.

1. Introduction

Both activated water with permanent magnets (Ignatov, Mosin, 2014) and solenoids (Liu et al., 2022) are applied in agriculture. Results have been obtained with magnetic induction parameters of B=500 and 1000 Gauss. The results, conducted on sheep, have demonstrated changes in daily and total milk production. The milk composition was improved. The ewes and lambs have improvement of hematological and biochemical parameters (Shamsaldain, 2012). The magnetic field exposure increases the shelf life of goat milk (Wei et al., 2022). Scientific studies show that adding potassium carbonate to the diet increases the synthesis of milk fats in cows (Alfonso-Aliva et al., 2017). Carbohydrates provided can lead to fermentation, acidification, and a decrease in pH in the digestive system of domestic animals (Krause, Oetzel, 2006; Emery, Brown, 1961). An alkaline environment improves the alkaline balance in the digestive system and reduces inflammatory diseases (Jenkins et al., 2014). In 2015, the possibility of combining water with potassium carbonate was indicated (Fraley et al., 2015). The studies and analyses aim to demonstrate the spectral parameters of potassium carbonate and water activated with a magnetic field. Based on the spectral peaks, the corresponding bio-effects of the obtained results are illustrated.

* Corresponding author
E-mail addresses: mbioph@abv.bg (I. Ignatov)

2. Materials and Methods

2.1. Spectral Methods

2.1.1. Non-equilibrium Energy Spectrum (NES) and Differential Non-equilibrium Energy Spectrum (DNES)

Antonov and co-authors created a device for the research with NES and DNES spectral methods (Antonov et al., 1989; Todorova, Antonov, 2000; Ignatov, Mosin, 2014). In the hermetical camera, the water evaporated. Antonov described the effect of discreet evaporations of water drops. The device studies the wetting angle θ of the water drops.

During the process of the evaporation of the water drops, the wetting angle changes discreetly. The dependence between the wetting angle and the average energy of the hydrogen bonds is the following:

$\Theta = \arccos(-1+bE)$, where $b = I(1+\cos\theta_o)/C\gamma o$ (1)

The range of the parameters of the hydrogen bonds is the following:

E=(-0.0912)-(-0.1387) eV; 736-1117 cm^{-1}; λ = 8.9 – 13.6 μm

In (1) θ is the wetting angle, and b is a temperature-dependent parameter. E is the energy of hydrogen bonds between the oxygen atom of one water molecule and the hydrogen of another (Gramatikov et al., 1992; Kumbhakkhane et al., 2013).

The function f(E)is estimate as *energy distribution spectrum*. A non-equilibrium process of evaporation of water droplets is energy spectrum of water. The value of NES and DNES is eV^{-1}. (Antonov, 1995; Todorova, Antonov, 2000).

DNES is the difference between the NES spectrum of water sample and NES of control water sample.

Δf(E)=f(water sample)-f(control water sample) (2)

DNES is studied in eV^{-1}

DNES is measured in eV^{-1}, f(*) marks the evaluated energy

The methods NES and DNES were applied for the investigations of natural water (Todorov et al., 2010; Ignatov, Valcheva, 2023) and solutions of plants (Ignatov, Popova, 2021; Ignatov et al., 2022).

2.1.2. Fourier transform infrared spectroscopy

Fourier-IR spectrometer Brucker Vertex was used for the research of IR-spectra of potassium carbonate.

Thermo Nicolet Avatar 360 Fourier-transform IR has the following parameters: average spectral range: 370-7800 cm^{-1}; visible spectral range 2500-8000 cm^{-1}; permission: 0.5 cm^{-1}; accuracy of wave number: 0.1 on 2000 cm^{-1}

2.2. Scheme for 1000 L water influenced with permanent magnetic field and dissolve potassium

Figure 1 illustrates a scheme for 1000 L water influenced by a permanent magnetic field and dissolved potassium carbonate

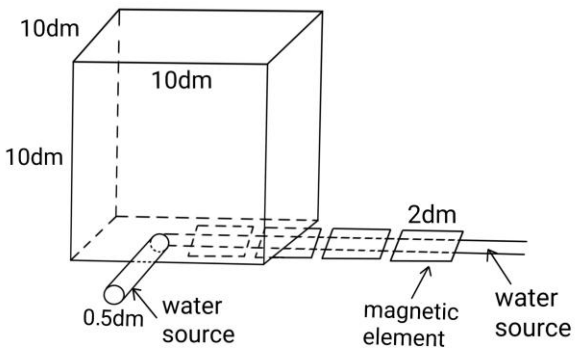

Fig. 1. Scheme for 1000 L water influenced by a permanent magnetic field and dissolved potassium carbonate

Drinking water comes from a water source located where flocks of sheep and goats are raised. The water pipe is placed in permanent magnets. Each magnet has a length of 20 cm. The magnetically activated water flows through the source with a diameter of 5 cm into the troughs for the domestic animals to drink. Sheep and goats drink 7-10 L per day. One container for a day can provide fresh water for 100-140 animals. It is constantly replenished, allowing the water to be influenced by magnetic field.

2.3. Parameters of the magnetic field for influence on water

The induction B of 1 cm from the surface of one element from Figure 1 is 1000 Gauss with a magnetic moment of 0.002 A.m².

3. Results and Discussion

3.1. Results with Potassium Carbonate

3.1.1. Research of water solution of K_2CO_3

Potassium carbonate dissociates into K^+ and CO_3^{2-} ions in solution:

$K_2CO_3 \rightarrow 2K^+ + CO_3^{2-}$

CO_3^{2-} reacts with water (H_2O) to form carbonic acid (H_2CO_3)

$CO_3^{2-} + H_2O \rightarrow HCO_3^- + OH^-$

HCO_3^- can react again with water:

$HCO_3^- + H_2O \rightarrow H_2CO_3 + OH^-$

Potassium carbonate with a molar concentration of 0.1 M or concentration of 13.82 $g.L^{-1}$ has pH=11.5

With 0.1 M or 13.82 $g.L^{-1}$, the concentration of the hydroxide ions (OH^-) is $3.16.10^{-3}$ M:

$pOH=-\log(3.16.10^{-3})=2.5$

$pH=14-pOH=11.5$

With 0.01 M or 1.382 $g.L^{-1}$, the concentration of the hydroxide ions (OH^-) is $3.16.10^{-4}$ M:

$pOH=-\log(3.16.10^{-4})=3.5$

$pH=14-pOH=10.5$

With 0.001 M or 0.1382 $g.L^{-1}$, the concentration of the hydroxide ions (OH^-) is $3.16.10^{-5}$ M:

$pOH=-\log(3.16.10^{-5})=4.5$

$pH=14-pOH=9.5$

With 0.0001 M or 0.01382 $g.L^{-1}$, the concentration of the hydroxide ions (OH^-) is $3.16.10^{-6}$ M:

$pOH=-\log(3.16.10^{-6})=5.5$

$pH=14-pOH=8.5$

For the volume 1000 L with 13.8 g, the pH=8.5

3.1.2. IR Fourier Spectral Analysis of K_2CO_3

Figure 2 shows the results with IR Fourier Spectral Analysis of K_2CO_3.

Figure 2 has the following spectral peaks in the range of NES spectrums.

(-E) of 0.1049 eV or (λ=11.82 μm; $\tilde{\nu}$=846 cm^{-1})

(-E) of 0.1095 eV or (λ=11.33 μm; $\tilde{\nu}$=883 cm^{-1})

(-E) of 0.1312 eV or (λ=9.45 μm; $\tilde{\nu}$=1058 cm^{-1})

3.2. Spectral Analysis of Water Influenced with Permanent Magnetic Field

Water samples were used as an object of this influence for the research on the effects of permanent magnetic field. The control samples were with the same deionized water without the influence of the magnetic field.

The mathematical model was created for the percent distribution of water molecules according to the parameters of the energies (-E) of hydrogen bonds (Ignatov, Mosin, 2014) (Ignatov, Gluhchev, 2021).

Table 1 and Figure 3 illustrate the results.

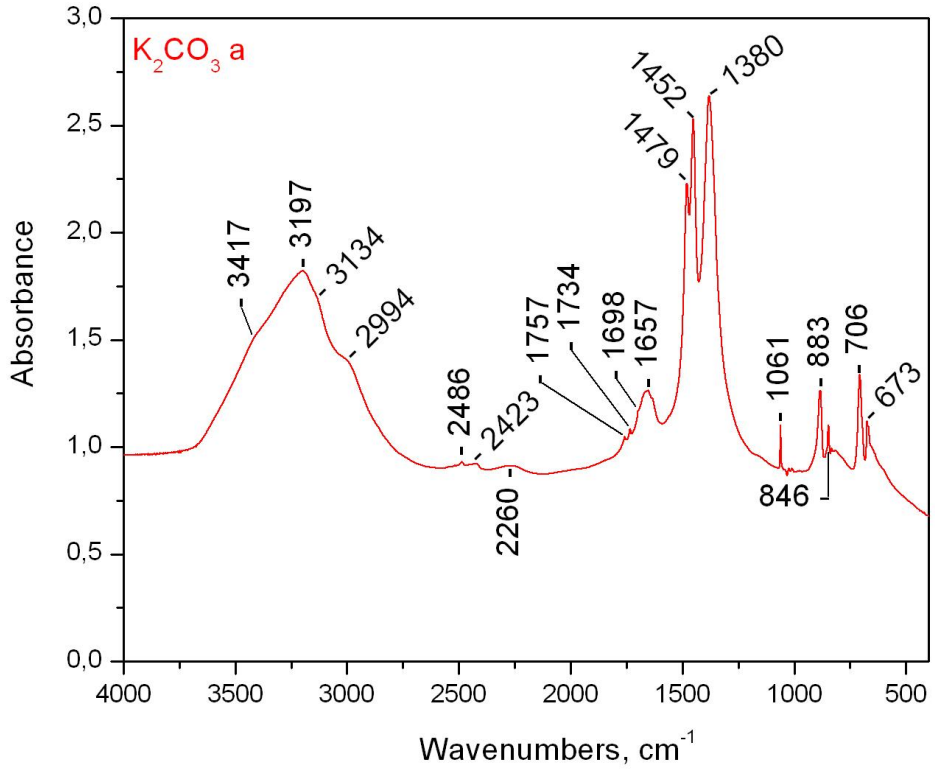

Fig. 2. Results with IR Fourier Spectral Analysis of K_2CO_3

Table 1. Mathematical models of samples influenced with magnetic field with 1000 G and control samples

-E(eV) x-axis	Deionized Water Influenced by Magnetic Field (%((-E_{value})/ (-$E_{total\ value}$)	Deionized Water Control sample (%((-E_{value})/(-$E_{total\ value}$)
0.0937	0	0
0.0962	4.5	6.3
0.0987	9.1	6.3
0.1012	4.5	6.3
0.1037	4.5	3.2
0.1062	0	3.2
0.1087	0	10.7
0.1112	18.2	0
0.1137	13.7	4.3
0.1162	0	0
0.1187	0	6.3
0.1212	4.5	6.3
0.1237	0	6.3
0.1262	0	10.7
0.1287	13.7	8.7
0.1312	0	0
0.1337	9.1	10.7
0.1362	4.5	10.7
0.1387	13.7	0

With t-test of Student for 10 samples and 10 control samples the result is statistically relable for $p<0.05$

In the NES spectrum of water treated with a permanent magnetic field with induction B=1000 Gauss, there are the following peaks:

(-E) of 0.1112 eV or (λ=11.15 μm; ṽ=897 cm^{-1})

(-E) of 0.1137 eV or (λ=10.91 μm; ṽ=917 cm^{-1})

(-E) of 0.1287 eV or (λ= 9.63 μm; ṽ= 1038 cm^{-1})

(-E) of 0.1387 eV or (λ=8.95 μm; ṽ=1117 cm^{-1})

Notes:

E=-0.1112 eV; λ=11.15 μm; 897 cm^{-1} is the local extremum for the conductivity of calcium (Ca^{2+}) ions (Zhang et al., 2018; Ignatov et al., 2023).

E= -0.1387 eV; λ=8.95 μm; 1117 cm^{-1} is the local extremum for the restructuring of water molecules with the highest energies of hydrogen bonds for the configurations of water clusters from 16 to 24 water molecules (Neshev et al., 2022).

There are wavenumbers of hexagonal water clusters with different positions of water molecules for n=6. The basic wavenumber is 1117 cm^{-1} (Heine et al., 2013).

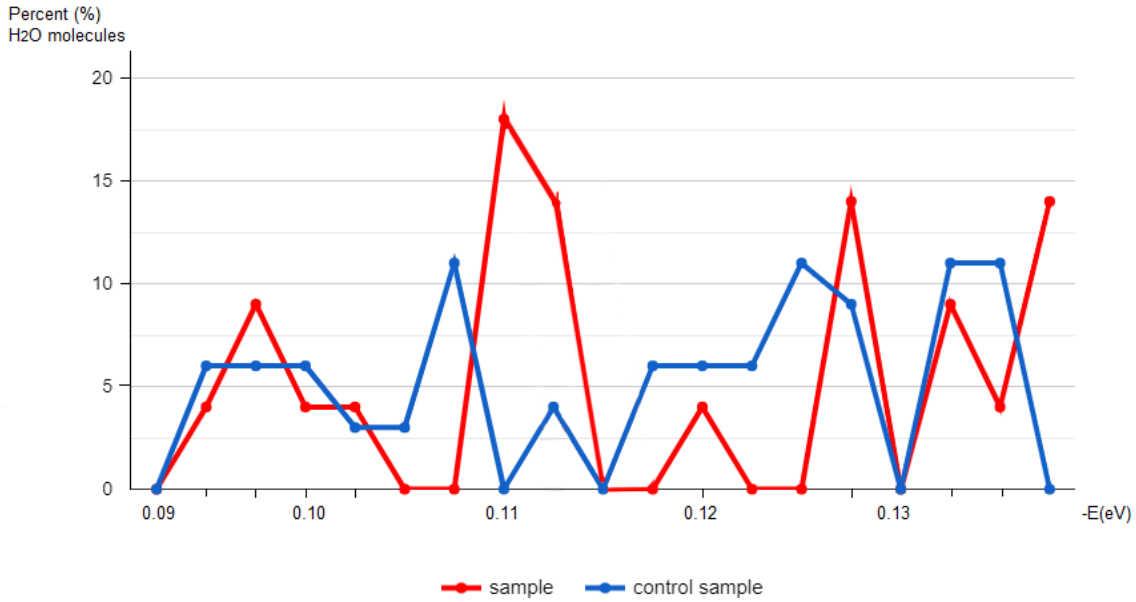

Fig. 3. Percent distribution of water molecules according to the values of (-E) of hydrogen bonds

A scientific team headed by Mehandjiev showed theoretically with calculations with Gaussian distribution that the maximal number of water clusters must have averge energy of hydrogen bonds between water molecules of (-E) of 0.1137 eV or (λ=10.91 μm; ṽ=917 cm-1) (Mehandjiev et al., 2022). The research shows that ṽ =917 for the hydrogen-bonded molecules (Brooker et al., 2022).

The obtained water meets the standards set forth in Ordinance No 9/2001, Official State Gazette, issue 30, and Decree No 178/23.07.2004 of Council of Ministers, Bulgaria. Notably, regulations do not encompass potassium, carbonate, and hydrogencarbonate ions. These ions are not governed by any specific limits or restrictions. (Ignatov, 2020).

4. Conclusion

The research provides compelling evidence that enhancing water properties through exposure to a permanent magnetic field and introducing potassium carbonate leads to notable improvements in the quality of milk and dairy products sourced from cows, sheep, and goats.

This novel approach, involving a 1000-liter plastic container treated with a permanent magnetic field and dissolved potassium carbonate, creates an alkaline environment within the container. One of the effects is on the gastric acidity of animals and conferring protection against various diseases.

Employing advanced spectral methods, including Non-equilibrium Energy Spectrum (NES), Differential Non-equilibrium Energy Spectrum (DNES), and Infrared (IR) Fourier Spectral Analysis, the investigations were carried out on deionized water, serving as a representative model system.

The spectral results show that the joint effect of the magnetic field and potassium carbonate is connected with the following peaks for the wave numbers

$\tilde{\nu}$=846; 883; 897; 917; 1038; 1058; 1117 cm^{-1}

The extrapolated results, encompassing a volume of 1000 liters or 1 ton of drinking water, demonstrated compliance with relevant regulations regarding drinking water quality.

Notably, potassium, carbonate, and hydrogencarbonate ions were found to be exempt from a regulatory limit of reactions. Furthermore, the studies of different authors established significant alterations in key parameters for sheep, goats, and cows. The parameters were daily and total milk production, milk composition, and hematological and biochemical factors. The scientists were proved the effects on ewes and growth.

The extension of the shelf life of goat milk under the influence of the magnetic field is an intriguing discovery with potential implications for dairy production.

Additional investigations revealed that that incorporating potassium carbonate into the cows, goat, and sheep diet fosters increased synthesis of milk fats.

However, it is essential to note that introduction of carbohydrates may lead to process such as fermentation, acidification, and pH reduction within the digestive systems of domestic animals. Creating an alkaline environment is beneficial in maintaining an alkaline balance and mitigating inflammatory conditions.

In summary, this research underscores the potential of magnetic field-activated water and potassium carbonate as influential factors in enhancing agricultural and animal husbandry practices and dairy production quality.

The combination of the spectral analyses for the quality of water for cows, sheep, and goats and practical applications holds promise for future advancements in the field of animal husbandry.

References

Alfonso-Aliva et al., 2017 – *Alfonso-Aliva, A.L. et al.* (2017). Potassium carbonate as a cation source for early-lactation dairy cows fed high-concentrate diets. *J. Dairy Sci.* 100: 1751-1765.

Antonov, 1995 – *Antonov, A.* (1995). Research of the non-equilibrium processes in the area of allocated systems, Dissertation thesis for degree “Doctor of Physical Sciences”, Blagoevgrad, Sofia, 1-255.

Antonov et al., 1989 – *Antonov, A., Yuskesselieva, L., Teodossieva, I.* (1989). Influence of ions on the structure of water under conditions far away from equilibrium. *Physiologie.* 26: 2552.

Brooker et al., 1989 – *Brooker, M. H.* (1989). *A* Raman frequency and intensity studies of liquid H_2O, $H_2{}^{18}O$ and D_2O. *J Raman Spectrosc.*

Emery, Brown, 1961 – *Emery, R. S., Brown, L. D.* (1961). Effect of feeding sodium and Potassium bicarbonate on milk fat, rumen pH, and volatile fatty acid production. *J. Dairy Sci.* 44: 1899-1902.

Fraley et al., 2015 – *Fraley, S. E. et al.* (2015). Effect of variable water intake as mediated by dietary potassium carbonate supple-mentation on rumen dynamics lactating dairy cows. *J. Dairy Sci.* 98: 3247-3256.

Gramatikov et al., 1992 – *Gramatikov, P., Antonov A, Gramatikova M.* (1992). Study of the Properties and structure variations of water systems under the stimulus of outside influences. *Fresenius Z. Anal. Chem.* 343: 134-135.

Heine et al., 2013 – *Heine, N., Fagiani, M. R., Rossi, M. et al.* (2013). Isomer-selective detection of Hydrogen-bond vibrations in the protonated water hexamer. *J. Am. Chem. Soc.* 135, 22: 8266-8273.

Ignatov, Mosin, 2014 – *Ignatov, I., Mosin, O.V.* (2014). Structural Mathematical models describing water clusters. *Nanotechnology Research and Practice.* 3: 141-158.

Ignatov, Mosin, 2014 – *Ignatov, I., Mosin, O.V.* (2014). Basic concepts of magnetic water treatment. *European Journal of Molecular Biotechnology*. 4: 72-85.

Ignatov, 2020 – *Ignatov I.* (2020). Standards for researching and registering drinking mineral and mountain spring waters in Bulgaria. *Asian Journal of Chemical Sciences*. 9: 12-18.

Ignatov, Popova, 2021 – *Ignatov, I., Popova, T.P.* (2021). Applications of Moringa oleifera Lam., Urtica dioica L., Malva sylvestris L. and Plantago major L. containing potassium for recovery. *Plant Cell Biotechnol Mol Biol J*. 22(7-8): 22: 93-103.

Ignatov, Gluhchev et al., 2021 – *Ignatov, I., Gluhchev, G., Neshev, N., Mehandjiev, D.* (2021). Structuring of water clusters depending on the energy of hydrogen bonds in electrochemically activated waters anolyte and catholyte. *Bulg. Chem. Commun.* 53(2): 234-239.

Ignatov, et al., 2023 – *Ignatov, I., Iliev, M.T, Gramatikov, P. et al.* (2023). Non-equilibrium processes in the atmosphere, water, and reactions with calcium carbonate in the environment. *J. Chem. Technol. Metall.* 58(6).

Ignatov, Valcheva, 2023 – *Ignatov, I., Valcheva, N.* (2023). Physicochemical, isotopic, spectral, and microbiological analyses of water from glacier Mappa, Chilean Andes. *J. Chil. Chem. Soc.* 68(1): 5802-5906.

Jenkins et al., 2014 – *Jenkins et al.* (2014). Addition of potassium carbonate to continuous cultures of mixed ruminal bacteria shifts fatty acids and daily production of biohydrogenation intermediates. *J Dairy Sci.* 97: 975-984.

Krause, Oetzel, 2006 – *Krause, K.M., Oetzel, G.R.* (2006). Understanding and preventing subacute ruminal acidosis in dairy herbs. A review. *Anim. Feed Sci. Technol.* 126: 215-236.

Kumbharkhane et al., 2013 – *Kumbharkhane, A., Joshi, Y. S., Mehrotra, S. C. et al.* (2013). Study of hydrogen bonding and thermodynamic behavior in water–1,4-dioxane mixture using time domain reflectometry. *Physic B: Condensed Matter*. 421: 1-7.

Liu et al., 2022 – *Liu, Zh. et al.* (2017). The sterilization effect of solenoid magnetic field direction on heterotrophic bacteria in circulating cooling water. *Procedia Engineering*. 174: 1296-1302.

Mehandjiev et al., 2022 – *Mehandjiev, D., Ignatov, I., Neshev, N. et al.* (2022). Formation of clusters in water and their distribution according to the number of water molecules. *Bulg. Chem. Commun*. 54(3): 211-216.

Neshev, Toshkova et al., 2022 – *Neshev, N., Ignatov, I., Toshkova, R. et al.* (2022). Hydrogen bonds energy distribution and information-theoretic analysis of blood serum from hamsters with experimental Graffi tumor. *Libri Oncologici*. 50(2-3): 52-61.

Shamsaldain, 2012 – *Shamsaldain, R.* (2012). Effect of magnetic water on productive efficiency of Awassi sheep. *Iraqi Journal of Veterinary Sciences*. 2: 75-82.

Todorov et al., 2010 – *Todorov, S., Damianova, A., Antonov, A. et al.* (2010). Investigations of natural waters spectra from the Rila Mountain National Park lakes. *Comptes Rendus de l 'Academie Bulg. des Sci*. 63: 555-560.

Todorova, Antonov, 2000 – *Todorova, L. Antonov, A.* (2000). Note on the drop evaporation method for studying water hydrogen bond distribution: An Application to filtration. *Comptes Rendus de l 'Academie Bulg. des Sci*. 53(7): 43-46.

Ordinance No. 9, 2001 – Ordinance No. 9. Methods for evaluating physicochemical and microbiological indicators according to Ordinance No. 9/2001, Official State Gazette, issue 30, and decree No. 178/23.07.2004 regarding the quality of water intended for drinking and household purposes, 2001.

Wei et al., 2022 – *Wei Jia, Min Zhang, Mudan Xu, Lin Shi* (2022). Novel strategy to remove the odor in goat milk: Dynamic discovery magnetic field treatment to reduce the loss of phosphatidylcholine in a flash vacuum from the proteomics perspective. *Food Chemistry*. 375: 131889.

Zhang et al., 2018 – *Zhang et al.* (2018). Facilitated transport of CO_2 through the transparent and flexible cellulose membrane promoted by fixed-site carrier. *ACS Appl. Mater. Interfaces*. 10(29).

Published in the USA
European Journal of Molecular Biotechnology
Issued since 2013.
E-ISSN: 2409-1332
2022. 10(1): 15-21

DOI: 10.13187/ejmb.2022.1.15
https://ejmb.cherkasgu.press

Complex Extraction of Surfactant Proteins from the Farm Animal Lungs Using a Non-Ionic Detergent Tween 20

Pavel A. Krylov [a, b, *], Alexey K. Surin [c, d], Mariya Yu. Suvorina [e], Valery V. Novochadov [a, *]

[a] Volgograd State University, Russian Federation
[b] Laboratory of the Genomic and Postgenomic Technologies, Federal Scientific Centre of Agroecology Complex Meliorations and Protective Afforestation, Russian Academy of Sciences, Volgograd, Russian Federation
[c] Biological Testing Laboratory, Branch of the Shemyakin–Ovchinnikov Institute of Bioorganic Chemistry, Russian Academy of Sciences, Pushchino, Russian Federation
[d] Laboratory of the Biochemistry of Pathogenic Microorganisms, State Research Centre for Applied Microbiology and Biotechnology, Obolensk, Russian Federation
[e] Laboratory of Bioinformatics and Proteomics, Institute of Protein Research, Russian Academy of Sciences, Pushchino, Russian Federation

Abstract

The article presents the pilot extraction technology of surfactant proteins, represented by hydrophilic (SP-A, SP-D) and hydrophobic (SP-B, SP-C) fractions from bovine and porcine lungs. Borate buffer, tris buffer, and phosphate buffer saline solution were the basis for extraction solutions. Twin 20 was applied in various concentrations as a mild detergent capable of preserving the spatial structure of the protein. To identify and give a semi-quantify estimation of surfactant protein presence in extracts we used one-dimensional electrophoresis and mass spectrometry technique. A semi-quantitative assessment of the protein concentration using integrated density on electrophoregrams showed that the borate buffer allows us to isolate the largest amount of SP-A, and the tris buffer SP-D without adding Tween 20 proved analogue effect if we perform extraction from the bovine lungs. Phosphate buffered saline solution + 1 % Tween 20 demonstrated the best efficiency of extraction of SP-A and SP-D from porcine lungs. The extract solution of Tris-buffer + Tween 20 content demonstrated the highest efficiency, and Phosphate-buffered saline + 1 % Tween 20 was the least effective, failing to isolate SP-C. The detergent addition was critical to the degree of surfactant proteins extraction. The development of a comprehensive technology for the extraction of surfactant proteins will reduce the cost and laboriousness of their production. This technology will make it possible to reduce the cost of surfactant-based drugs and make them more accessible to the population.

Keywords: protein extraction, surfactant proteins, nonionic detergents, Tween 20, lungs, farm animals.

1. Introduction

Today, there is an increasing need in creating technologies aimed at obtaining a larger number of proteins and other functional compounds from various objects of plant and animal origin, reducing the prime and labor costs of the final product (Faustino et al., 2019).

* Corresponding author
E-mail addresses: p.krylov.volsu@yandex.ru (P.A. Krylov)

Currently, of particular interest is the development of a surfactant protein (SP) complex extraction. SPs play an important role in medicine, as being used for the treatment of pulmonary diseases such as respiratory distress syndrome, acute lung injury syndrome, and oncology (Casals et al., 2012, Lopez-Rodriguez et al., 2014, Bayat et al., 2015, Fedorchenko et al., 2016, Cheung et al., 2017). Interest in SPs has increased due to the pandemic caused by SARS-CoV-2. Some hypotheses say that SARS-CoV-2 may cause an intense loss of surfactant proteins (Takano, 2020, Avdeev et al., 2021) and that the exogenous surfactant proteins may assist in the recovery of damaged alveoli and prevent severe acute respiratory failure (Ghati et al., 2021).

Pulmonary surfactant is a lipid: protein complex containing four proteins dipalmitoyl-phosphatidylcholine as the major component. The pulmonary SPs family includes four types of proteins. Hydrophilic SP-A a is of 5.3 % and SP-D is of 0.6 % of all SPs, hydrophobic SP-B is of 0.7 % and SP-C is of 0.4 % of ones. All SPs are synthesized by alveolar type II cells (Chroneos et al., 2010). The lipid complex includes phosphatidylcholine as the predominant species (70-80 %) and neutral lipids as cholesterol (5-8 %). Among these, the saturated dipalmitoyl-phosphatidylcholine accounts for 40 % in average whereas unsaturated phosphatidylcholine and anionic phospholipids as phosphatidylglycerol (8 %) and phosphatidylinositol (PI) are also important components (Cañadas et al., 2020).

Such surfactant-based drugs as synthetic Exosurf (Glaxo-Wellcome, USA-UK) and ALEK (Britannica, UK), semi-synthetic Surfactant-TA (TokyoTanabe, Tokyo, Japan) and Survanta (AbbVie Inc, Chicago, USA), natural Curosurf, (Chiesi Farmaceutici, Farma, Italy), Infasurf (Forrest Labs, St. Louis, USA), CLSE (Rochester, NY, USA), and Surfactant-HL and Surfactant-BL, (Russia) are known to be the most popular in clinical practice. Synthetic surfactants demonstrate less effective, although they are certainly more available (Patel, 2018). At the same time, these drugs, unlike natural ones, do not contain SPs. This fact is extremely important for their properties, which are crucial for surfactant phospholipid ability to reduce surface tension at the phase boundary (alveolar surface – air), while synthetic drugs, including Exosurf, do not contain these proteins.

Currently, existing technologies allow us to distinguish all four isoforms of SPs, but such techniques are suitable only for research tasks. There is currently no way to isolate all SPs for further purification and use as medicines. Most of the existing technologies are based on the Bligh and Dyer method including Russian developments (Beers et al., 1992, Strong et al., 1998, Rozenberg et al., 2019). They are very laborious and expensive because it is necessary to carry out additional stages of lung homogenate purification. Nonionic detergents are the best choice for membrane protein isolation. Tween 20 (TW20), one of them, is highly soluble in water. With the hydrophilic-lipophilic balance of 16.7, TW20 gently destroys lipid bilayer membranes, preventing protein denaturation, and has the lowest critical micelle concentration of 0.06 compared to other detergents from this group (Seddon et al., 2004, Johnson, 2013).

This study aims to develop a pilot technology for the complex extraction of all 4 surfactant protein isoforms from bovine and porcine lungs using the non-ionic detergent TW 20.

2. Materials and methods

We used bovine and porcine lungs as raw materials.

The lungs were immediately frozen at -20°C after the removal, then transported to the laboratory and prepared for the extraction of SPs and further mass spectrometric studies (Cox et al., 2006).

2.1. Surfactant protein extraction

The protocol included lung washing in cold PBS for 1 hour in a reciprocating shaker. The lung samples were homogenized in 15 ml of extraction solution (Table 1) per gram of tissue using an Ultra-Turrax Tube Drive homogenizer (IKA, Germany) and glass beads in a BMT-20 S/G tube for 5 minutes at 5000 rpm.

Next, we centrifuged the samples at 700g for 5 min in a ScanSpeed Mini centrifuge (Labogene, Denmark). The protein concentration in the supernatant was determined by the Lowry method. The obtained samples were divided into two parts: the first part was used for SDS-PAGE, the second part was placed in cryovials and frozen at -80°C in an MDF-C8V1 freezer (Sanyo, Japan) for subsequent mass spectrometry analysis.

Table 1. Extraction solutions

Base	Concentration	pH	Detergent
Tris-buffer	10 mM	7.4	None or 0.1 % TW20 or 1 % TW20
Borate buffer	10 mM	9.18	
PBS (Phosphate buffer+0,9% NaCl)	-	7.4	

2.2. SDS-PAGE

We performed one-dimensional SDS-polyacrylamide gel electrophoresis to separate and identify extracted proteins in a Mini-PROTEAN Tetra Cell (BIO-RAD, USA) under denaturing conditions using SDS according to the Laemmli method and 10-250 kDa markers, Precision Plus Protein™ Unstained Protein Standards (BIO-RAD, USA). The obtained protein fractions were mixed with sample buffer (SB-buffer) in a ratio of 1:10 and thermostated at 95°C for 5 minutes. The stacking (5 %) and resolving (12 %) gel solutions were prepared for electrophoresis. After electrophoresis, the gels were placed in a gel-fixing solution for 15 minutes, stained with Coomassie Brilliant Blue G-250 (Russia, Dia-M) for an hour, and then placed in a gel-washing solution overnight. Then the gels were soaked for 15-60 minutes in ddH_2O, and the ChemiDoc™ Touch Imaging System (BIO-RAD, USA) used to captured and make digital images (Ruano et al., 1998). A semi-quantitative assessment of the surfactant protein concentration in the gels was carried out using ImageJ 1.53K software (NIH, USA) by measuring the integrated density. SP-A detected in 28-36 kDa range (Kankavi et al., 2004), SP-D had mass of 43 kDa (Crouch et al., 1994), SP-B had mass 8 kDa as monomeric form and of 16 kDa as dimeric form (Simonato et al., 2011), and SP-C one detected in 3.7-21 kDa range (Beers et al., 2017).

2.3. Mass spectrometry

2.3.1. Sample preparation

The preliminarily purification of sample hydrolysates from urea concluded in hydrophobic chromatography using ZipTip microcolumns (Millipore, Germany) with C_{18} resin. After being applied to the microcolumn, the samples were washed with 4 % acetonitrile solution (Merck, Germany) and 0.1 % trifluoroacetic acid (PanReac AppliChem, Germany) in deionized water. The definitive washing of peptides was conducted on the column with 80 % acetonitrile solution and 0.1 % trifluoroacetic acid and drying on a vacuum concentrator.

2.3.2. Mass spectrometry protocol

The first stage of analysis concluded in applying the hydrolysate of analyzed samples on a reversed-phase column with subsequent peptide separation in an acetonitrile gradient. The peptides eluted from the column entered the ionization chamber, where the ions were analyzed by tandem mass spectrometry on an Orbitrap Elite ETD high-resolution mass spectrometer (Thermo Scientific, Germany). Ion fragmentation was carried out by two independent methods HCD and CID.

2.3.3. Data analysis

During mass spectrometry we obtained sets of peptide and ion fragment masses and processed them using a commercial program PeakStudio 7.5. (Bioinformatics Solutions Inc, Canada). Then we identified peptides using the UniProt database. Protein identification was considered reliable if the value of the identification confidence level -10 lgP was ≥ 20.

2.4. Statistical Processing

We processed quantitative data in the Statistica 12.0 (StatSoft Inc., USA) with indicator calculations used to characterize nonparametric samples in biomedical studies: the normality of the distribution, the median [1st quartile, 3rd quartile] and assessed the significance of sample differences. We also used the Mann-Whitney test with a p-value less than 0.05 to analyze the differences between two independent samples.

3. Results

The eluting solutions showed different results in the dependence of animal species, buffer kind, and TW20 concentration. Figure 1 demonstrates that the complex extraction of SPs let to the highest protein output from porcine lungs in cases of PBS with 0.1 % TW20 and 1 % TW20

application. If we took bovine lung samples the using borate buffer with 0,1 % TW20 provided the best result. The addition of Tris-buffer in 1 % concentration let to worse protein outcome, 3-4 times less compared to other buffers.

Figure 2 presents the results of electrophoresis application to identify the concrete SPs in obtained samples from bovine lungs (2A) and porcine lungs (2B). We can see small peaks on the electropherogram of bovine lung extracts at the 37 kD marker level corresponding to the mass of an SP-A monomer, in case of borate buffer, borate buffer + 0.1 % TW20, and tris-buffer without detergent revealed at first, second, and fourth tracks, accordingly.

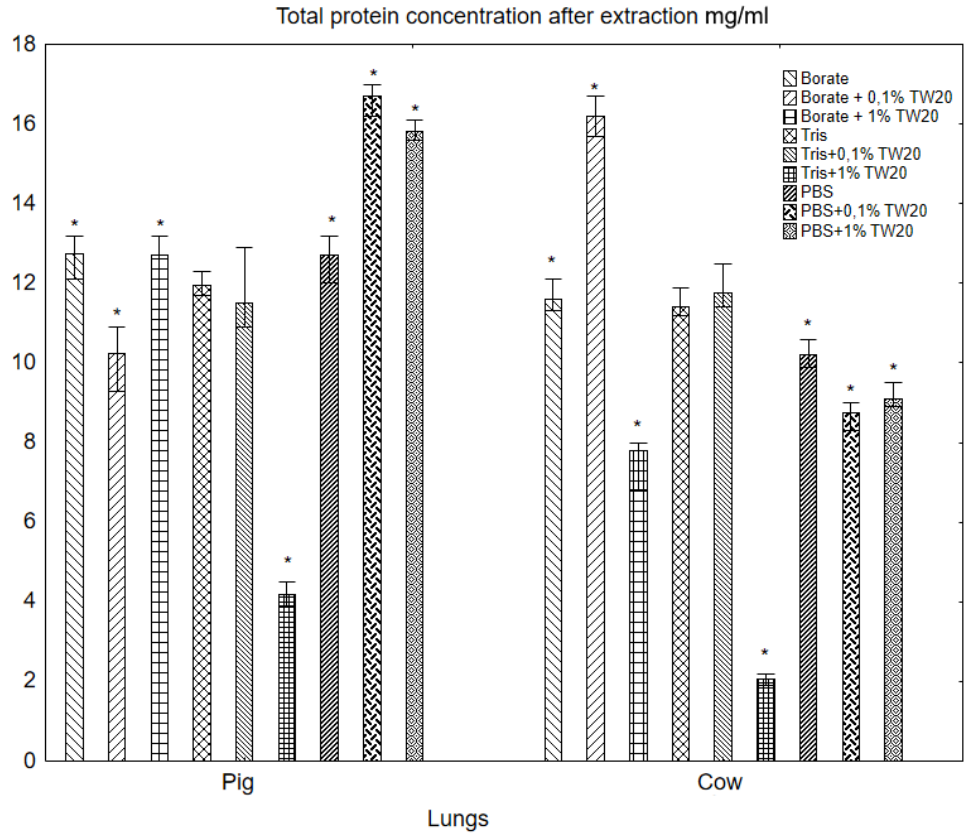

Fig. 1. Total protein concentration in the samples obtained by different extraction solutions. * – statistically significant differences (nonparametric Mann-Whitney test, $p < 0.05$)

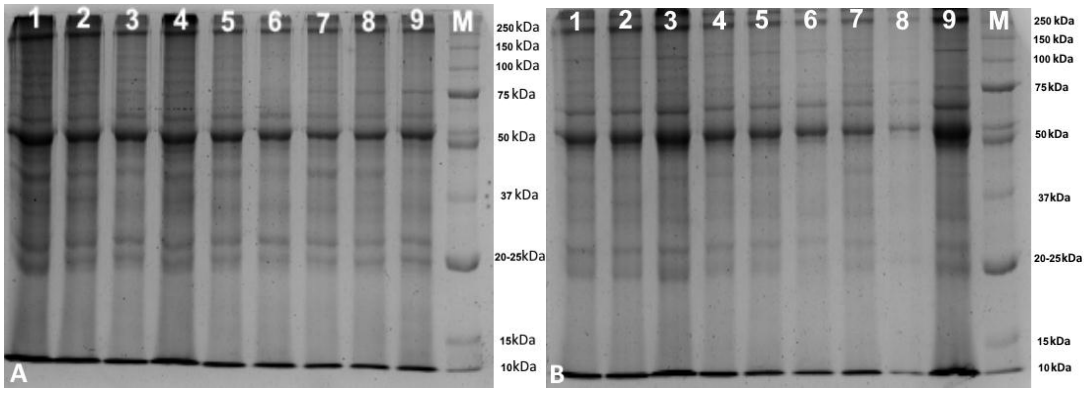

Fig. 2. SDS-PAGE electropherogram of bovine lung (A) and porcine lung (B) extracts. Coomassie Brilliant Blue G-250 staining, 1:10 dilution. Protein bands: 1 – Borate, 2 – Borate + 0.1 % TW20, 3 – Borate + 1 % TW20, 4 – Tris, 5 – Tris + 0,1 % TW20, 6 – Tris + 1 % TW20, 7 – PBS, 8 – PBS + 0,1 % TW20, 9 –PBS + 1 % TW20, 10 – BIO-RAD protein markers.

In all tracks we see an electrophoretic strip between the 37 kDa and 50 kDa markers, presumably appropriating SP-D. No peaks corresponding to the dimeric form of SP-B were found, but it is possible that the monomeric form is on a peak at the 10 kDa marker. All sample tracks have a blurred strip at the 20-25 kDa marker corresponding to different SP-C.

On the electropherogram of porcine lung extracts we can see three blurry peaks at the 37 kD marker level corresponding to the mass of an SP-A, in a case of borate buffer + 0.1 % TW20, borate buffer + 1 % TW20, and PBS + 1 % TW20 revealed at second, thirdly and ninth tracks, accordingly. In all tracks except for PBS + 0,1 % TW20, we see an electrophoretic strip between the 37 kDa and 50 kDa markers, presumably appropriating SP-D. The electrophoretic strip corresponding to the dimeric form of SP-B is not revealed on electropherogram porcine lung extracts. Probably SP-C is present in an electrophoretic strip corresponding to the 10 kDa marker, but all sample tracks, except for PBS + 0.1 % TW20, have a strip at the 20-25 kDa marker corresponding to SP-C preform.

Table 2 presents an estimate of the integrated density of electrophoretic strips obtained by extraction with different eluents. This indicator made it possible to select six samples for mass spectrometric analysis and protein identification.

These samples were represented by extract SPs, obtained in PBS + 1 % TW20, borate buffer + 0.1 % TW20, and tris-buffer of bovine lungs and porcine lungs. The flattening electrophoretic strip did not allow the evaluation of integrated density for the hydrophobic fraction of SPs.

Mass spectrometry allowed identifying all SPs in experimental samples. The results of mass spectrometry are consistent with electropherograms. They prove the presence of all hydrophobic and hydrophilic SPs in the electrophoretic strip corresponding to molecular markers. The extraction solution containing PBS + 1% TW20 made it possible to isolate only three SPs from the lung extracts of bovine and porcine. Mass spectrometry revealed SPs in porcine lung and bovine lungs extracts, but also to other closely related mammalian species.

Table 2. SDS-PAGE analysis of SPs for each solvent-detergent extraction

Solvent	Concentration TW 20	Protein	Integrated Density	
			Bovine lungs samples	Porcine lungs samples
PBS	0 %	SP-A SP-D	0,60 0,73	0,79 0,78
	0,1 %	SP-A SP-D	0,57 0,71	0,82 0,83
	1 %	SP-A SP-D	0,60 0,70	0,96 0,95
Borate buffer	0 %	SP-A SP-D	0,96 0,85	0,87 0,89
	0,1 %	SP-A SP-D	0,78 0,89	0,94 0,91
	1 %	SP-A SP-D	0,66 0,77	0,67 0,68
Tris-buffer	**0 %**	SP-A SP-D	0,77 0,94	0,82 0,86
	0,1 %	SP-A SP-D	0,74 0,73	0,78 0,80
	1 %	SP-A SP-D	0,58 0,66	0,72 0,69

This result may be associated with a low degree coverage of amino acid sequences from 1 % to 8 %, and a low significant value. The SP-A extracted with tris-buffer without TW20 from porcine lung sample had highly identified (-10 lgP 36.62) with an amino acid sequence coverage of 10 %. The use of borate buffer + 0.1 % TW20 allowed the isolation of SP-A from bovine lungs to have a high degree identity (-10 lgP 118.31) and an amino acid sequence coverage of 21 %. Figure 2 presents the electrophoretic strips corresponding to molecular markers 21 kDa and therefore SP-C. It should be noted for separation of the hydrophilic SPs to be more successful compared to ones.

The results of mass spectrometry and electrophoresis confirm the fact, that all SPs fractions were isolated during extraction by various eluting solutions.

4. Discussion

We choose the TW20 detergent because it has a gentle action on cell lipids. It destructs lipid-lipid and lipid-protein interactions and preserves native protein structure and function. In addition, TW20 has the best physicochemical properties compared to other detergents from the nonionic group, like Triton-x100. On the other hand, it is necessary to find a way to purify the obtained extracts from TW20 (Seddon et al., 2004) before using them in developing drugs based on SPs.

Porcine lung fat percentage is much higher than in bovine lungs. These differences affect the quality of extraction and the effectiveness of the detergent, resulting in extraction degree. Ionic strength and pH may also be effective (Ruano et al., 1998). An alkalization can lead to the destruction of lipids (Spilling et al., 2013), which we can observe in protein extraction from the porcine lung. The dimeric form of SP-B was absent, and this fact indicates the breaking hydrophobic bond between the molecules after the detergent addition, and the presence of hydrophobic proteins was confirmed by the mass spectrometry.

Since mass spectrometry analysis involved the use of a complete database of all protein sequences of the studied organisms, commonly we see in the samples major plasma proteins such hemoglobin, albumins, immunoglobulins, etc. Particularly, its presence reduced the quality of the analysis. In future, the purification from the major proteins of blood plasma over 60 kDa may improve the quality of SPs identification in extracts.

5. Conclusion

The use of extraction solutions based on borate buffer and PBS with 0.1 % and 1 % TW20 makes it possible to isolate more proteins from the bovine and porcine lung extracts. However, SP-C and/or SP-D may be absent in some samples if non-effective eluting formula was used. Tris-based extraction buffer with and without TW20 seems to be most effective for isolating all fractions of SPs, which confirmed by the results of mass spectrometry. To sum up, we can state that it is necessary to use tris-buffer as the main solvent for further modification and optimization of the complex SPs extraction.

6. Acknowledgements

The reported study was funded by RFBR according to the research project № 18-44-343003 “Complex potentially bioactive molecules isolation, based on the study of cattle lungs proteome”.

References

Avdeev, 2021 – *Avdeev, S.N., Trushenko, N.V., Chikina, S.Y. et al.* (2021). Beneficial effects of inhaled surfactant in patients with COVID-19-associated acute respiratory distress syndrome. *Respiratory Medicine*. 185: 106489. DOI: 10.1016/j.rmed.2021.106489

Bayat et al., 2015 – *Bayat, S., Porra, L., Broche, L. et al.* (2015). Effect of surfactant on regional lung function in an experimental model of respiratory distress syndrome in rabbit. *Journal of Applied Physiology*. 119(3): 290-298. DOI: 10.1152/japplphysiol.00047.2015

Beers et al., 2017 – *Beers, M.F., Nureki, S.I., Mulugeta, S.* (2017). The role of epithelial cell quality control in health and disease of the distal lung, in: V.K. Sidhaye, M. Koval (Eds.). Lung Epithelial Biology in the Pathogenesis of Pulmonary Disease, Academic Press, New York. Pp. 133-163. DOI: 10.1016/B978-0-12-803809-3.00008-7

Beers et al., 1992 – *Beers, M.F., Bates, S.R., Fisher, A.B.* (1992). Differential extraction for the rapid purification of bovine surfactant protein B. *The American Journal of Physiology*. 262(6 Pt 1): L773-L778. DOI: 10.1152/ajplung.1992.262.6.L773

Cañadas et al., 2020 – *Cañadas, O., Olmeda, B., Alonso, A., Pérez-Gil, J.* (2020). Lipid-protein and protein-protein interactions in the pulmonary surfactant system and their role in lung homeostasis. *International Journal of Molecular Sciences*. 21(10): 3708. DOI: 10.3390/ijms 21103708

Casals et al., 2012 – *Casals, C., Cañadas, O.* (2012). Role of lipid ordered/disordered phase coexistence in pulmonary surfactant function. *Biochimica et Biophysica Acta*. 1818(11): 2550-2562. DOI: 10.1016/j.bbamem.2012.05.024

Cheung et al., 2017 – *Cheung, C.H-Y., Juan, H.-F.* (2017). Quantitative proteomics in lung cancer. *Journal of Biomedical Science*. 24(1): 24-37. DOI: 10.1186/s12929-017-0343-y

Chroneos et al., 2010 – *Chroneos, Z.C., Sever-Chroneos, Z., Shepherd, V.L.* (2010). Pulmonary surfactant: an immunological perspective. *Cellular Physiology and Biochemistry: International Journal of Experimental Cellular Physiology, Biochemistry, and Pharmacology*. 25(1): 13-26. DOI: 10.1159/000272047

Cox et al., 2006 – *Cox, B., Emili, A.* (2006). Tissue subcellular fractionation and protein extraction for use in mass-spectrometry-based proteomics. *Nature protocols*. 1(4): 1872-1878. DOI: 10.1038/nprot.2006.273

Crouch et al., 1994 – *Crouch, E., Persson, A., Chang, D. et al.* (1994). Molecular structure of pulmonary surfactant protein D (SP-D). *The Journal of Biological Chemistry*. 269(25): 17311-17319.

Faustino et al., 2019 – *Faustino, M., Veiga, M., Sousa, P. et al.* (2019). Agro-food byproducts as a new source of natural food additives. *Molecules*. 24(6): 1056. DOI: 10.3390/molecules24061056

Fedorchenko et al. 2016 – *Fedorchenko, K.Y., Ryabokon', A.M., Kononikhin, A.S. et al.* (2016). The effect of space flight on the protein composition of the exhaled breath condensate of cosmonauts. *Russian Chemical Bulletin*. 65(11): 2745-2750. DOI: 10.1007/s11172-016-1645-z

Ghati et al., 2021 – *Ghati, A., Dam, P., Tasdemir, D. et al.* (2021). Exogenous pulmonary surfactant: A review focused on adjunctive therapy for severe acute respiratory syndrome coronavirus 2 including SP-A and SP-D as added clinical marker. *Current Opinion in Colloid & Interface Science*. 51: 101413. DOI: 10.1016/j.cocis.2020.101413

Johnson, 2013 – *Johnson, M.* (2013). Detergents: Triton X-100, Tween-20, and More. *Materials and Methods*. 3: 163. DOI: 10.13070/mm.en.3.163

Kankavi et al., 2004 – *Kankavi, O., Roberts, M.S.* (2004). Detection of surfactant protein A (SP-A) and surfactant protein D (SP-D) in equine synovial fluid with immunoblotting. *Canadian Journal of Veterinary Research = Revue canadienne de recherche veterinaire*. 68(2): 146-149.

Lopez-Rodriguez et al., 2014 – *Lopez-Rodriguez, E., Pérez-Gil, J.* (2014). Structure-function relationships in pulmonary surfactant membranes: from biophysics to therapy. *Biochimica et Biophysica Acta*. 1838(6): 1568-1585. DOI: 10.1016/j.bbamem.2014.01.028

Patel, 2018 – *Patel, A.* (2018). Recombinant synthesis of pulmonary surfactant proteins SP-B and SP-C. *Aston University*. 263.

Rozenberg, 2019 – *Rozenberg, O.A., Sejliev, A.A.* (2019). Method for obtaining surfactant from bovine lungs, RU 2 691 648 C1, Date of publication: 17.06.2019 Bull. № 17.

Ruano et al., 1998 – *Ruano, M.L., Pérez-Gil, J., Casals, C.* (1998). Effect of acidic pH on the structure and lipid binding properties of porcine surfactant protein A. Potential role of acidification along its exocytic pathway. *The Journal of Biological Chemistry*. 273(24): 15183-15191. DOI: 10.1074/jbc.273.24.15183

Seddon et al., 2004 – *Seddon, A.M., Curnow, P., Booth, P.J.* (2004). Membrane proteins, lipids and detergents: not just a soap opera. *Biochimica et Biophysica Acta*, 1666(1-2): 105-117. DOI: 10.1016/j.bbamem.2004.04.011

Simonato et al. 2011 – *Simonato, M., Baritussio, A., Ori, C. et al.* (2011). Disaturated-phosphatidylcholine and surfactant protein-B turnover in human acute lung injury and in control patients. *Respiratory Research*. 12(1): 36. DOI: 10.1186/1465-9921-12-36

Spilling et al., 2013 – *Spilling, K., Brynjólfsdóttir, Á., Enss, D. et al.* (2013). The effect of high pH on structural lipids in diatoms. *J Appl. Phycol.* 25: 1435-1439. DOI: 10.1007/s10811-012-9971-5

Strong et al., 1998 – *Strong, P., Kishore, U., Morgan, C. et al.* (1998). A novel method of purifying lung surfactant proteins A and D from the lung lavage of alveolar proteinosis patients and from pooled amniotic fluid. *Journal of Immunological Methods*. 220(1-2): 139-149. DOI: 10.1016/s0022-1759(98)00160-4

Takano, 2020 – *Takano, H.* (2020). Pulmonary surfactant itself must be a strong defender against SARS-CoV-2. *Medical Hypotheses*. 144: 110020. DOI: 10.1016/j.mehy.2020.110020